www.czasopisma.pan.pl PAN POLSKA AKADEMIA NAUK www.journals.pan.pl

Archives of Environmental Protection
Vol. 44 no. 2 pp. 55–61

PL ISSN 2083-4772
DOI 10.24425/119691

DE G DE GRUYTER OPEN

Leaching of heavy metals from MSWI fly ash: experiments vs. simulation

Qili Qiu, Xuguang Jiang*, Zhiliang Chen, Shengyong Lu, Mingjiang Ni

Institute for Thermal Power Engineering
Zhejiang University, China

*Corresponding author's e-mail: jiangxg@zju.edu.cn

Keywords: Simulation, MSWI fly ash, microwave, hydrothermal treatment, Visual MINTEQ.

Abstract: In this work, pH-dependence experiments and leaching modeling using Visual MINTEQ were performed to evaluate the stability and simulate the leaching characteristics of heavy metals in municipal solid waste incineration (MSWI) fly ash. Modeling the equilibrium concentration of Cd, Cu, Cr, Ni, Pb and Zn in raw and treated fly ash was the main target and was conducted over a pH range of 0.5–14. In addition, simulation of the leaching behavior of MSWI fly ash with different additives was also conducted. The treated fly ash was solidified by a microwave-assisted hydrothermal process with added phosphate. The initial elemental concentrations of MSWI fly ash, including raw and treated fly ash, were detected by a microwave apparatus and inductively coupled plasma atomic emission spectroscopy (ICP-AES). The ICP-AES analysis showed that most leaching concentrations of treated fly ash decreased considerably compared to the raw fly ash. The simulation results indicated that the dissolution/precipitation simulation models of Zn, Cu and Pb were broadly consistent with the experimental results, while the leaching behaviors of Ni, Cr and Cd were determined by both dissolution/precipitation and surface complexation mechanisms. In addition, the models of reagent solidification revealed that the stabilization effect of Na_2S was better than that of Na_2CO_3. This model will be useful in the evaluation of the leaching concentrations of heavy metals in fly ash.

Introduction

As of 2014, the amount of municipal solid waste incineration reached 5.33×10^7 tons in China, accounting for 32.5% of the disposed total MSW (2015). Thus, a large quantity of fly ash was accumulated with a high toxicity of heavy metals (Xue et al. 2009, Anastasiadou et al. 2012) and dioxins (Pan et al. 2013). Cement solidification (Shi and Kan 2009), chemical stabilization (Zhao et al. 2002, Sukandar et al. 2009) and thermal treatment (Tu et al. 2007, Yang et al. 2008), including hydrothermal treatment (Jin et al. 2013, Hu et al. 2015) are the main means of fly ash disposal at present. In China, HJ/T300−2007 (Solid Waste-Extraction Procedure for Leaching Toxicity-Acetic Acid Buffer Solution Method) was selected as the standard procedure to evaluate the leaching toxicity of heavy metals in fly ash. The pH of the extraction buffer was 2.64 ± 0.05. The leaching concentration of heavy metals varied with different leaching methods, in the order of HJ/T300−2007> TCLP > HJ/T299-2007 (Solid Waste-Extraction Procedure for Leaching Toxicity--Sulphuric Acid & Nitric Acid Method). It is widely accepted that pH plays an important role in the leaching behavior of heavy metals. Therefore, it is necessary to assess the leaching behavior of heavy metals in fly ash.

The chemical equilibrium program Visual MINTEQ was developed by the U.S. environmental protection agency (EPA). This program is of great use for calculating the equilibrium mass distribution in mixing, dilution, multiple solid phases, adsorption, etc. The software contains a powerful equilibrium constant database, including liquid-phase complexation, dissolution/precipitation, oxidation/reduction, gas-liquid equilibrium balance reactions, adsorption reactions, etc. The Visual MINTEQ model has been applied to simulate metal leaching behaviors in contaminated soils (Houben et al. 2012), sludge (Karamalidis and Voudrias 2008) and fly ash (Eighmy et al. 1995, Bhattacharyya and Reddy 2012), for which it includes a sequential toxicity characteristic leaching procedure and pH-dependence test (Zhang et al. 2008); the model has also been applied to simulate other waste material (Li et al. 2001). Additionally, this procedure has been used in practical engineering applications to evaluate and predict the emissions from a road built with MSWI bottom ash (Aberg et al. 2006). Zhang et al. (Zhang et al. 2008) reported that the leaching behaviors of Pb and Cd in raw MSWI fly ash were controlled by a dissolution/precipitation mechanism, while Zn and Ni were affected by surface adsorption reactions. Nevertheless, little research has been reported on the leaching behavior of treated fly ash after hydrothermal processing or other treatments. MSWI fly ash was successfully solidified using microwave-assisted hydrothermal methods in our previous work (Qiu et al. 2016, Qiu et al. 2016). To evaluate the stability and simulate the leaching characteristics of heavy metals, pH-dependence experiments and leaching modeling using Visual MINTEQ were conducted.

The objective of this work was to model the leaching equilibrium concentrations of Cd, Cu, Cr, Ni, Pb and Zn of raw and treated fly ash using the data from experimental results in the pH-dependence leaching test. The long-term behaviors of

the soluble metals can be understood and described well with the help of the leaching models. In addition, this model can be used to predict the leaching concentrations of fly ash in the leaching tests at a certain pH (Fernandez-Olmo et al. 2007).

Materials and methods

Materials

Several amounts of MSWI fly ash were gathered from the dedusting installation (fabric filter) of an incinerator plant located in Zhejiang province, with an 800-ton daily capacity. The flue gas treatment involved spray neutralization, including a hydrated lime suspension and activated carbon suspension. The samples were dried for 24 h at 105°C, before being used for the following detection and experiments.

Microwave-assisted hydrothermal process

The dried fly ash was mixed with Na_2HPO_4 (1.5 mol/kg, Na_2HPO_4/fly ash) and deionized water (3 mL/g, water/fly ash). Then, the mixtures were heated in a microwave apparatus (Sineo MDS-6, China) for 20 min at 200°C. After this procedure, the solid (treated fly ash) was cooled, centrifuged, collected and dried. Microwave-assisted hydrothermal process was applied to solidify the heavy metals of the MSWI fly ash samples in this study, and afterwards, the raw and treated samples were used in pH-dependence tests.

pH-dependence test

The pH-dependence test experiments were conducted in parallel at various pH levels (1-13) of both raw and treated fly ash. HNO_3 and NaOH were used to obtain leaching solutions with different H^+ concentrations. The mixture of fly ash and leaching solution at a liquid/solid ratio of 20 ml/g was shaken for 18 ± 2 h at a speed of 30 ± 2 rpm. Then, the mixtures were filtered through a 0.6−0.8 μm borosilicate glass fiber filter after centrifuging. Finally, the filtrate was detected by ICP-AES (ICP−AES, Thermo Scientific XII, USA) to obtain the leaching concentration of heavy metals. Notably, the pH values in the experiments were tested and recorded at the end of the leaching procedure to compare with the leaching models.

Leaching modeling

Visual MINTEQ (v 3.1) was used to calculate the leaching concentrations of Cd, Cr, Cu, Ni, Pb and Zn at variable pH values of the raw and treated fly ash samples. The equilibrium speciation model was based on precipitation/dissolution/complexation equilibrium reactions. The initial mass concentrations of each component (Cd^{2+}, Cr^{3+}, Cu^{2+}, Ni^{2+}, Pb^{2+}, Zn^{2+}, Ca^{2+}, PO_4^{3-}, SO_4^{2-}, Cl^-, etc.) were obtained after the pH-dependence experiment. The pH value in the simulation models was fixed during the whole leaching process. This model was set to simulate and predict the leaching behavior of MSWI fly ash after the microwave-assisted hydrothermal process. Furthermore, this program was also used to simulate the solidification effect of S^{2-} and CO_3^{2-} on fly ash in this work.

Results and discussion

Initial concentration of raw and treated fly ash

The elemental initial concentrations of the MSWI fly ash are listed in Table 1. These data were the maximum leaching concentrations of fly ash, which were gained determined at relatively low pH conditions. Most leaching concentrations from the treated fly ash were found to be significantly decreased compared to those in the raw samples. Therefore, the microwave-assisted hydrothermal process operated on fly ash, which led to a low leaching concentration of heavy metals in treated fly ash.

Leaching behavior of raw and treated MSWI fly ash at various pH values

The experimental and simulation results of the leaching behavior are shown in Fig. 1 for both raw and treated MSWI fly ash. The leaching concentration of heavy metal ions was obviously affected by the solution pH and sharply decreased at a certain pH (Cho et al. 2005).

Zn. For raw fly ash, Zn^{2+} precipitated mainly in the form of $Zn(OH)_2$ at pH 7.5–12.5. At pH 7.5, 70.9% Zn^{2+} was precipitated; meanwhile, the remainder basically existed in the state of free zinc ions. Furthermore, $Zn(OH)_2$ dissolved to the forms of $Zn(OH)_3^-$ and $Zn(OH)_4^{2-}$, as well as the leaching concentration of Zn at pH values over 13, and almost entirely existed as $Zn(OH)_4^{2-}$ under strong alkaline conditions. For the treated fly ash, the pH range of precipitation was extended. Zn^{2+}, $ZnSO_4$ (aq) and $ZnCl^+$ were the main forms of Zn in the strong acid solutions (pH 0–4). The formation of the $Zn_3(PO_4)_2$ precipitate started at pH 4, and the percentage of $Zn_3(PO_4)_2$ reached 98.628% when pH was 6. $Zn_3(PO_4)_2$ was substituted by $Zn(OH)_2$ in the pH range of 11–12. Above pH 12, $Zn(OH)_2$ started to dissolve, which did not consistently match the experimental results. Therefore, it can be concluded that more stable materials in basic solution were formed during the microwave-assisted hydrothermal process. Another point worth mentioning was that the precipitation of

Table 1. The initial elemental concentrations of MSWI fly ash (mg/L)

Element	Concentration		Element	Concentration	
	Raw	Treated		Raw	Treated
Ca^{2+}	9500	7846	Pb^{2+}	25.72	7.838
Mg^{2+}	374.28	348.4	Cd^{2+}	3.755	1.284
Al^{3+}	926.4	857.1	Cr^{3+}	12.46	3.455
Fe^{3+}	315.72	302.8	PO_4^{3-}	788	14499
Mn^{2+}	21.372	8.497	SO_4^{2-}	24.564	18.25
Zn^{2+}	138.1	61	AsO_4^{3-}	1.357	1.186
Cu^{2+}	189.6	61.2	Cl^-	289.6	37.2
Ni^{2+}	4.668	0.9814	F^-	9.1	8.9

The Proposed Place: Section 3.1

$Zn_3(PO_4)_2$ was not formed in the simulation results of raw fly ash because PO_4^{3-} preferentially combined with Ca ions in the form of $Ca_3(PO_4)_2$ precipitate. However, the concentration of PO_4^{3-} in treated fly ash was much higher, which contributed to the formation of a $Zn_3(PO_4)_2$ precipitate. Furthermore, the increased concentration of PO_4^{3} led to a lower Ca^{2+} concentration such that less soluble zeolite products of Ca ions were formed after treatment. Hence, the existence of excess PO_4^{3-} proved beneficial to the solidification of heavy metals.

Cu. The simulation results showed that $Cu_2(OH)_3Cl$ was the main form of Cu in raw fly ash at pH 5.5–6.5. Over 99% of the Cu existed as $Cu(OH)_2$ at pH 7–13, and meanwhile, $Cu(OH)_2$ was dissolved and the concentration of $Cu(OH)_3^-$ and $Cu(OH)_4^{2-}$ increased above pH 13. At pH 14, dissolved forms of Cu composed up to 18%. $CuHPO_4^-$ was formed in acidic conditions, accounting for approximately 92% of the total dissolved Cu ions at pH 5.5. For treated fly ash, the simulation results showed that $Cu_3(PO_4)_2$ was the main form at pH 4–8. Additionally, 59.5% and 90% of Cu was precipitated at pH 4 and pH 5, respectively. $Cu_3(PO_4)_2$ started to be transformed into $Cu(OH)_2$ at pH 8.5. Similarly, the precipitation of $Cu(OH)_2$ started to dissolve at pH 13. Additionally, no $Cu_3(PO_4)_2$ was found under acid conditions.

Pb. For the raw fly ash, $Pb_5(PO4)_3Cl$ started to precipitate at pH 2, and Pb^{2+} was almost totally transformed into precipitate at pH 3.5. $Pb(OH)_2$ existed as the main form of precipitation under basic conditions (pH 8.5–12.5). However, when pH was higher than 13, the precipitate dissolved to $Pb(OH)_3^-$. Thus, the leaching concentration of Pb also increased above pH 13, which was in concordance with the experimental results. With increasing PO_4^{3-} in treated fly ash, 66.9% precipitation was found at pH 1.5, which was lower than that in the raw fly ash. Additionally, as pH increased, $Pb(OH)_2$ formed and $Pb_5(PO4)_3Cl$ disappeared (pH 8–13). Compared with the results of raw and treated fly ash in the simulation or experimental results under the strong basic conditions (over pH 13), the treated one was more stable, with less Pb^{2+} leaching.

Thus, it was concluded that without considering adsorption reactions, the dissolution/precipitation simulation results of Zn, Cu and Pb were broadly in line with the experimental results. That is, the leaching behaviors of Zn, Cu and Pb were determined by the dissolution/precipitation mechanism. Heavy metals (Zn, Cu and Pb) in treated fly ash had high stabilities in the acidic and alkaline environments, as concluded from both experimental and simulation results.

Ni. For the raw fly ash, at pH 6–8, the simulation results were not in concordance with the results of the experiment, and the leaching concentration of the experiment was lower than the modeling results. It was suggested that Ni was solidified by surface complexation (adsorption), which led to a low leaching concentration in the pH-dependence experiment. Therefore, it was not explained well by the dissolution/precipitation model. However, at other pH ranges, the simulation results were coincident with the experimental results. Ni^{2+} was precipitated as the form of $Ni(OH)_2$, accounting for 72.1%, at pH 8. Additionally, at pH 12, the precipitate started to be dissolved as $Ni(OH)_3^-$, and there was approximately 10% Ni^{2+} dissolved in solution at pH 14. For the treated fly ash, it was shown that the deviation of the experimental and simulation results was very large at pH 2–9. The modeling results indicated that sufficient Ni^{2+} existed in solution at pH < 9, while the precipitation of Ni^{2+} to $Ni(OH)_2$ was initiated at a low pH value (pH 2) in the experiment and was completely converted to precipitate at pH 9. For the treated fly ash, the degree of deviation between the experimental and simulation results was greater in the pH range of 2–9, while in other pH ranges, the modeling results were in accordance with the experimental results. The production of the absorption area was due to the process of hydrothermal solidification, which contributed to the production of zeolites. Therefore, the solidification effect of the hydrothermal treatment proved indirectly.

Cr. The results of Cr were similar to those of the Ni analysis. The absorption area existed in the pH range of 1–6; meanwhile, at other pH ranges, the modeling results were consistent with the experimental results. The formed precipitate was $Cr(OH)_3$. At pH 13, the precipitate started to dissolve to form $Cr(OH)_4^-$.

Cd. Likewise, the absorption area appeared at pH 3–10. For the raw fly ash, the simulation results showed that approximately 16.8% of Cd precipitated at pH 9 as the form of $Cd_4(OH)_6SO_4$.However, the precipitation was converted to $Cd(OH)_2$ at pH 11–12.5. For the treated fly ash, $Cd_3(PO_4)_2$ and $Cd(OH)_2$ were the main forms of precipitation. It was indicated that the actual leaching concentration of both samples was decreased at a low pH because of the existence of the absorption reaction. In addition, above pH 13, the precipitate was dissolved into the forms of $Cd(OH)_3^-$ and $Cd(OH)_4^{2-}$.

Thus, it was concluded that the leaching behavior of Ni, Cr and Cd was determined by both the dissolution/precipitation mechanism and the surface complexation mechanism (adsorption). In our work, the adsorption reaction was not considered in the simulation. However, the treated fly ash via the microwave-assisted hydrothermal process was generally characterized by the adsorption. As a result, in the absorption area, the leaching behavior could not be explained using the dissolution/precipitation model, and in other pH ranges, the simulation results were consistent with the actual leaching behavior of heavy metals. The main production in leachate at pH 5 and 12 was simulated by Visual MINTEQ under the dissolution/precipitation mechanism. The results are shown in Tables 2 and 3.

Table 2. The main precipitate formed at pH 5 of the fly ash after stabilization with PO_4^{3-} (mol/L)

Precipitation	Equilibrium concentration	Precipitation	Equilibrium concentration
$MnHPO_4$(s)	3.0185E-04	Diaspore (AlO(OH))	3.4231E-02
Hydroxyapatite ($Ca_5(PO_4)_3(OH)$)	3.9070E-02	Hematite (Fe_2O_3)	2.7110E-03
$Zn_3(PO_4)_2{\cdot}4H_2O$ (s)	3.0106E-04	Plumbgummite ($PbAl_3(PO_4)2(OH)_5{\cdot}H_2O$)	3.7830E-05
$Cu_3(PO_4)_2$ (s)	3.1208E-02	Cr_2O_3 (c)	2.8248E-05
$MgHPO_4{\cdot}3H_2O$ (s)	6.0033E-03		

Table 3. The main precipitate formed at pH 12 of the fly ash after stabilization with PO_4^{3-} (mol/L)

Precipitation	Equilibrium concentration	Precipitation	Equilibrium concentration
Cupric Ferrite ($CuFe_2O_4$)	9.6299E-04	Diaspore (AlO(OH))	3.4254E-02
$Pb(OH)_2$ (s)	3.7814E-05	Cr_2O_3 (c)	3.2963E-05
$Cd(OH)_2$ (s)	1.1171E-05	MnHPO4(s)	3.0185E-04
Hydroxyapatite ($Ca_5(PO_4)_3(OH)$)	3.9152E-02	Brucite (Mg(OH)2)	1.4314E-02
$Ni(OH)_2$ (c)	1.6629E-05	Zincite (ZnO)	9.1920E-04
Hematite (Fe_2O_3)	1.7480E-03		

The Proposed Place: Section 3.2

(a) Raw

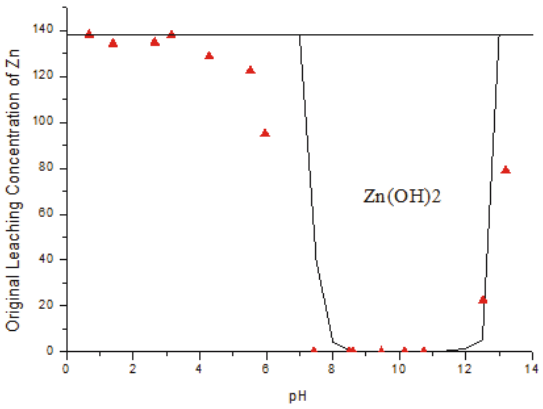

Treated

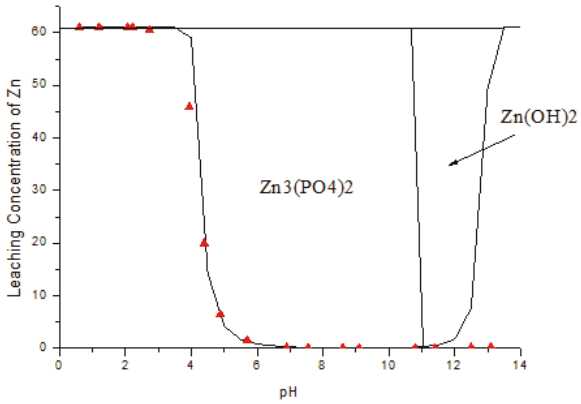

(b) Raw

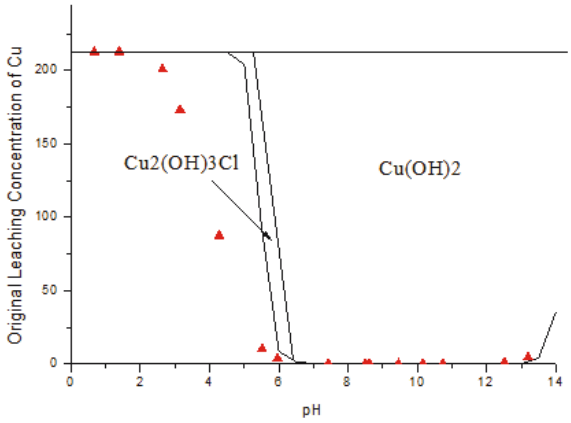

Treated

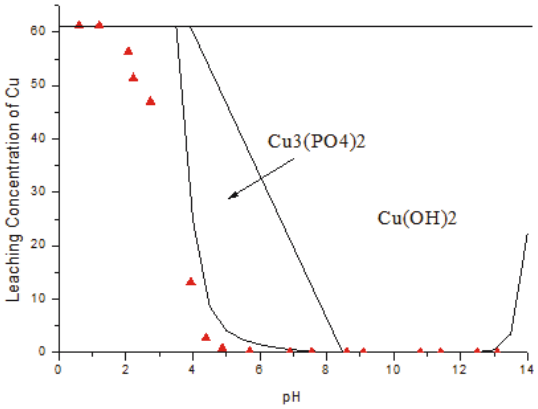

(c) Raw

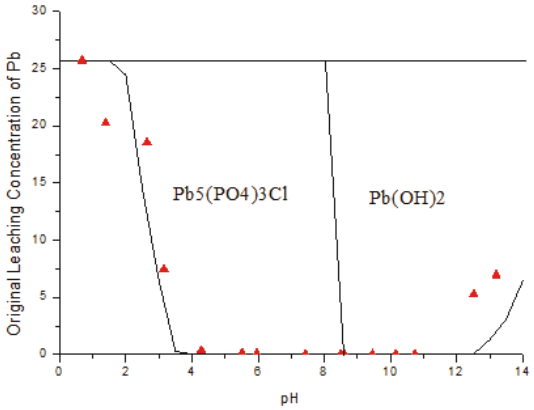

Treated

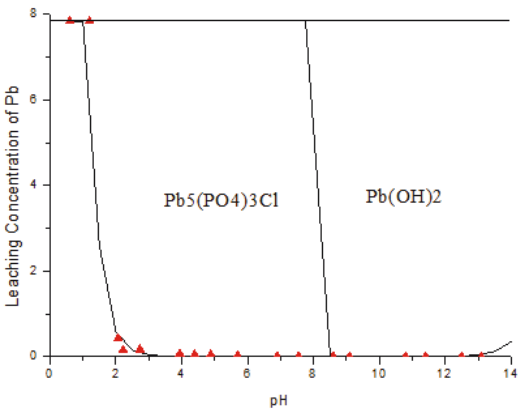

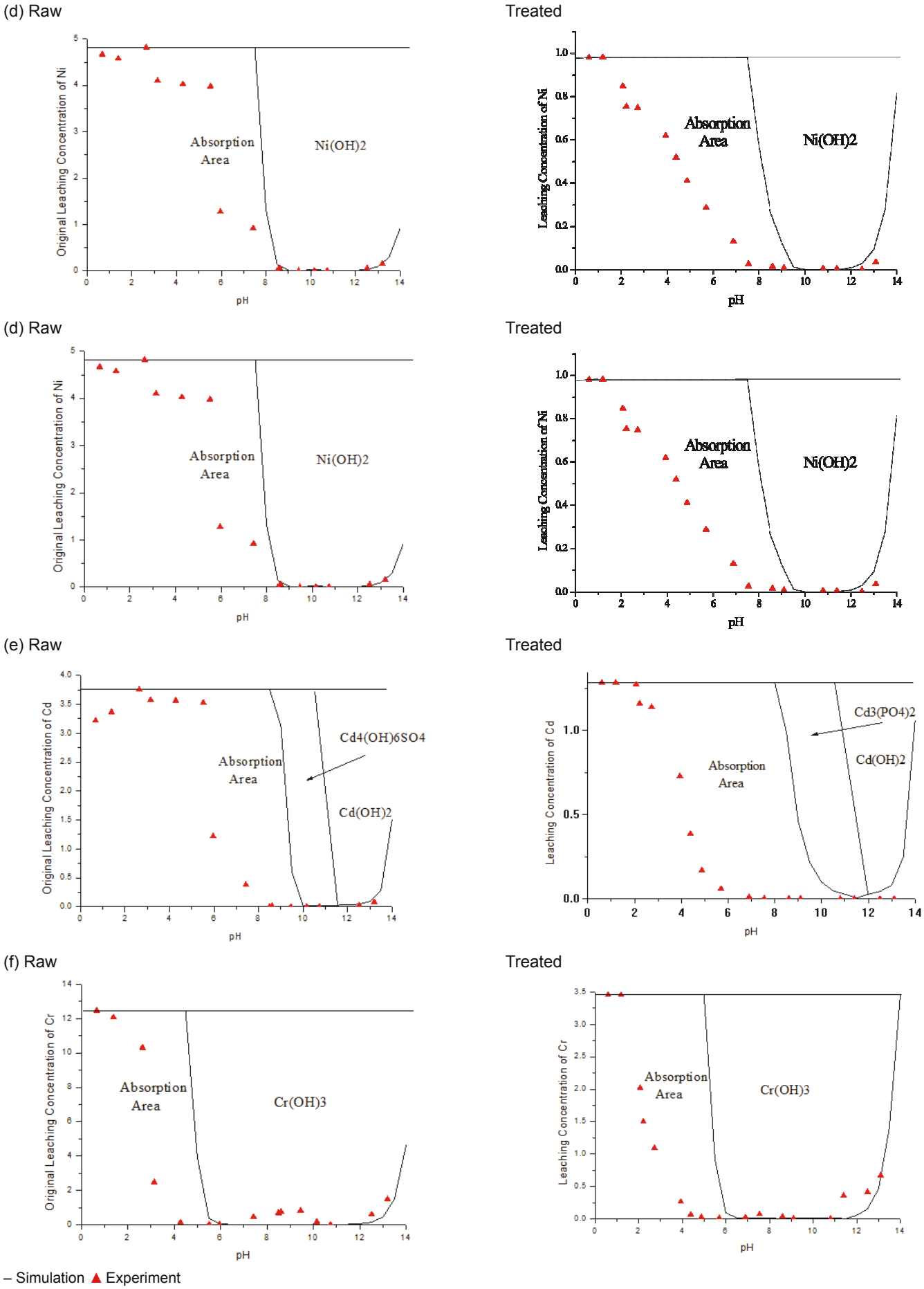

Fig. 1. Comparison between MINTEQ modeling result and experiment result of raw and treated MSWI fly ash (mg/L): (a) leaching concentration of Zn; (b) leaching concentration of Cu; (c) leaching concentration of Pb; (d) leaching concentration of Ni; (e) leaching concentration of Cd; (f) leaching concentration of Cr.

Simulation of leaching behavior of MSWI fly ash with different additives

Na_2S and Na_2CO_3 are usually selected as additives to stabilize the heavy metals in fly ash in the chemical stabilization or hydrothermal process. Therefore, simulation with added Na_2S and Na_2CO_3 was performed in this study.

The main production of the fly ash sample stabilized by 3% Na_2S in the leachate was simulated by Visual MINTEQ under the dissolution/precipitation mechanism, and the pH values were set at 5 and 12. The results are shown in Table 4 and Table 5.

At pH 5, the results showed that Cd, Cu, Ni, Pb and Zn were almost completely stabilized, while there was no change in Cr. That is, S^{2-} as a stabilizing agent could not decrease the leaching concentration of Cr. Meanwhile, at pH 12, the heavy metals (except Cr) of the treated fly ash remained stable and did not leach into the solution.

Additionally, the fly ash sample stabilized by 3% Na_2CO_3 was also simulated. However, the effect of stabilization was not as good as that of Na_2S. There was no effect on Pb and Cr in the leaching behavior. In addition, at pH 5, Cd, Cu, Ni and Zn continued to have a high leaching concentration. However, at pH 12, Cd, Cu, Pb and Zn stabilized, accounting for more than 99%. The precipitation results are listed in Table 6 and Table 7.

Table 4. The main precipitate formed at pH 5 of the fly ash after stabilization with Na_2S (mol/L)

Precipitation	Equilibrium concentration	Precipitation	Equilibrium concentration
Covellite (CuS)	2.9837E-03	Diaspore (AlO(OH))	3.4334E-02
Galena (PbS)	1.2413E-04	NiS (gamma)	7.9509E-05
Greenockite (CdS)	2.8619E-04	Sphalerite (ZnS)	2.1126E-03
Hydroxyapatite ($Ca_5(PO_4)_3(OH)$)	2.6362E-03	$Fe(OH)_{2.7}Cl_{0.3}$(s)	5.6533E-03
$MnHPO_4$(s)	3.5474E-04		

Table 5. The main precipitate formed at pH 12 of the fly ash after stabilization with Na_2S (mol/L)

Precipitation	Equilibrium concentration	Precipitation	Equilibrium concentration
Covellite (CuS)	2.9837E-03	Diaspore (AlO(OH))	3.4065E-02
Galena (PbS)	1.2414E-04	Cr_2O_3 (c)	1.1955E-04
Greenockite (CdS)	2.8621E-04	MnS (grn)	3.8882E-04
Hydroxyapatite $Ca_5(PO_4)_3(OH)$)	2.7657E-03	Brucite ($Mg(OH)_2$)	1.5394E-02
NiS (gamma)	7.9509E-05	$Ca_3(AsO_4)_2$:$4H_2O$(s)	4.5883E-06
Sphalerite (ZnS)	2.1126E-03	Ettringite $3CaO{\cdot}Al_2O_3{\cdot}{}_3CaSO_4{\cdot}32H_2O$)	8.4763E-05
Hematite (Fe_2O_3)	2.8267E-03	Portlandite ($Ca(OH)_2$)	2.5648E-02

Table 6. The main precipitate formed at pH 5 of the fly ash after stabilization with Na_2CO_3 (mol/L)

Precipitation	Equilibrium concentration	Precipitation	Equilibrium concentration
Chloropyromorphite(c) ($Pb_5(PO_4)_3Cl$)	2.4814E-05	Diaspore (AlO(OH))	3.4334E-02
$Fe(OH)_{2.7}Cl_{0.3}$(s)	5.6533E-03	Hydroxyapatite ($Ca_5(PO_4)_3(OH)$)	2.5969E-03
$MnHPO_4$(s)	3.8507E-04		

Table 7. The main precipitate formed at pH 12 of the fly ash after stabilization with Na_2CO_3 (mol/L)

Precipitation	Equilibrium concentration	Precipitation	Equilibrium concentration
Calcite ($CaCO_3$)	1.4143E-02	Diaspore (AlO(OH))	3.4065E-02
$Pb(OH)_2$(s)	1.2412E-04	Cr_2O_3 (c)	1.1955E-04
Hydroxyapatite ($Ca_5(PO_4)_3(OH)$)	2.7657E-03	Zincite (ZnO)	2.0976E-03
$Cd(OH)_2$(s)	2.8597E-04	Brucite ($Mg(OH)_2$)	1.5394E-02
Tenorite(c) (CuO)	1.5685E-04	$Ca_3(AsO_4)_2$:$4H_2O$(s)	4.5884E-06
$Ni(OH)_2$ (c)	7.9418E-05	Pyrochroite (MnO_2)	3.8026E-04
Ettringite ($3CaO{\cdot}Al_2O_3{\cdot}{}_3CaSO_4{\cdot}32H_2O$)	8.4763E-05	Portlandite($Ca(OH)_2$)	1.1573E-02
Cupric Ferrite ($CuFe_2O_4$)	2.8267E-03		

The purposed position: Section 4

As chemical stabilizers, the stabilization effect of Na_2S and Na_2CO_3 was determined by the precipitate dissolution balance mechanism between the heavy metals and the anions in reagents. Therefore, the treatment using chemical stabilization was more sensitive to pH compared to the hydrothermal process. The safety range of pH value of the latter was wider, with the effect of both adsorption and precipitation.

Conclusions

The pH-dependence experiments and leaching modeling using Visual MINTEQ were performed to evaluate the stability and to simulate the leaching characteristics of heavy metals in MSWI fly ash. Several conclusions are listed as follows:

(1) Compared to the raw fly ash, the leaching concentrations of metals in treated fly ash decreased significantly, which demonstrates the positive effect of the microwave-assisted hydrothermal treatment.
(2) The simulation results indicate that the dissolution/precipitation simulation models of Zn, Cu and Pb were consistent with the experimental results, while the leaching behaviors of Ni, Cr and Cd were determined by both the dissolution/precipitation mechanism and the surface complexation mechanism (adsorption).
(3) As reagent additives, Na_2S performed better than Na_2CO_3, with a greater decrease in heavy metals at the same pH.
(4) Visual MINTEQ can be used to predict the leaching concentrations of heavy metals in leaching tests and to obtain the precipitated production at a certain pH, which helps to illustrate the long-term leaching behavior description of fly ash or other waste materials.

Acknowledgements

This study was supported by the Innovative Research Groups of the National Natural Science Foundation of China (No. 51621005), the National Nature Science Foundation of China (No. 51676172), the Fundamental Research Funds for the Central Universities (No. 2016FZA4010), the Special Fund for the National Environmental Protection Public Welfare Program (Grant 201209023-4), and the Program of Introducing Talents of Discipline to University (Grant B08026).

References:

China Statistical yearbook (2015). China Statistics Press, Beijing, China 2015.

Aberg, A., Kumpiene, J. & Ecke, H. (2006). Evaluation and prediction of emissions from a road built with bottom ash from municipal solid waste incineration, *Science of the Total Environment*, 355, pp. 1–12.

Anastasiadou, K., Christopoulos, K., Mousios, E. & Gidarakos, E. (2012). Solidification/stabilization of fly and bottom ash from medical waste incineration facility, *Journal of Hazardous Materials*, pp. 165–170.

Bhattacharyya, P. & Reddy, K.J. (2012). Effect of flue gas treatment on the solubility and fractionation of different metals in fly ash of powder river basin coal, *Water Air Soil Pollution*, 223, pp. 4169–4181.

Cho, H., Oh, D. & Kim, K. (2005). A study on removal characteristics of heavy metals from aqueous solution by fly ash, *Journal of Hazardous Materials*, 127, pp. 187–195.

Eighmy, T.T., Eusden, J.D., Krzanowski, J.E., Domingo, D.S., Staempfli, D., Martin, J.R. & Erickson, P.M. (1995). Comprehensive approach toward understanding element speciation and leaching behavior in municipal solid waste incineration electrostatic precipitator ash, *Environmental Science & Technology*, 29, pp. 629–646.

Fernandez-Olmo, I., Lasa, C. & Irabien, A. (2007). Modeling of zinc solubility in stabilized/solidified electric arc furnace dust, *Journal of Hazardous Materials*, 144, pp. 720–724.

Houben, D., Pircar, J. & Sonnet, P. (2012). Heavy metal immobilization by cost-effective amendments in a contaminated soil: Effects on metal leaching and phytoavailability, *Journal of Geochemical Exploration*, 123, pp. 87–94.

Hu, Y., Zhang. P., Li, J. & Chen, D. (2015). Stabilization and separation of heavy metals in incineration fly ash during the hydrothermal treatment process, *Journal of Hazardous Materials*, 299, pp. 149–157.

Jin, Y.Q., Ma, X.J., Jiang, X.G., Liu, H. M., Li, X.D., Yan, J.H. & Cen, K.F. (2013). Effects of hydrothermal treatment on the major heavy metals in fly ash from municipal solid waste incineration, *Energy & Fuels*, 27, pp. 394–400.

Karamalidis, A.K. & Voudrias, E.A. (2008). Leaching behavior of metals released from cement-stabilized/solidified refinery oily sludge by means of sequential toxicity characteristic leaching procedure, *Journal of Environmental Engineering*, 134, pp. 493–504.

Li, X.D., Poon, C.S., Sun, H., Lo, I.M.C. & Kirk, D.W. (2001). Heavy metal speciation and leaching behaviors in cement based solidified/stabilized waste materials, *Journal of Hazardous Materials*, 82, pp. 215–230.

Pan, Y., Yang, L., Zhou, J., Liu, J. & Qian, G. (2013). Characteristics of dioxins content in fly ash from municipal solid waste incinerators in China, *Chemosphere*, 92, pp. 765–771.

Qiu, Q., Jiang, X., Lu, S. & Ni, M. (2016). Effects of microwave--assisted hydrothermal treatment on the major heavy metals of municipal solid waste incineration fly ash in a circulating fluidized bed, *Energy & Fuels*, 30, pp. 5945–5952.

Qiu, Q., Jiang, X., Lv, G., Lu, S. & Ni, M. (2016). Stabilization of heavy metals in municipal solid waste incineration fly ash in circulating fluidized bed by microwave-assisted hydrothermal treatment with additives, *Energy & Fuels*, 30, pp. 7588–7595.

Shi, H.S. & Kan, L.L. (2009). Leaching behavior of heavy metals from municipal solid wastes incineration (MSWI) fly ash used in concrete, *Journal of Hazardous Materials*, 164, pp. 750–754.

Sukandar, Padmi, T., Tanaka, M. & Aoyama, I. (2009). Chemical stabilization of medical waste fly ash using chelating agent and phosphates: Heavy metals and ecotoxicity evaluation, *Waste Management*, 29, pp. 2065–2070.

Tu, X., Yan, J., Ma, Z., Wang, Q., Cen, K. & Chéron, B. (2007). Vitrification of MSWI fly ash using thermal plasma technology, *Challenges of Power Engineering and Environment*, 1, pp. 823–826.

Xue, Y., Hou, H., Zhu, S. & Zha, J. (2009). Utilization of municipal solid waste incineration ash in stone mastic asphalt mixture: Pavement performance and environmental impact, *Construction and Building Materials*, 23, pp. 989–996.

Yang, Y., Xiao, Y., Voncken, J.H.L. & Wilson, N. (2008). Thermal treatment and vitrification of boiler ash from a municipal solid waste incinerator, *Journal of Hazardous Materials*, pp. 871–879.

Zhang, Y., Jiang, J. & Chen, M. (2008). MINTEQ modeling for evaluating the leaching behavior of heavy metals in MSWI fly ash, *Journal of Environmental Sciences*, 20, pp. 1398–1402.

Zhao, Y., Song, L. & Li, G. (2002). Chemical stabilization of MSW incinerator fly ashes, *Journal of Hazardous Materials*, B95, pp. 47–63.